



The temporal variability of oxygen inventory in the NE Black Sea slope water

Alexander G. Ostrovskii, Andrey G. Zatsepin, Vladimir A. Solovyev

Shirshov Institute of Oceanology, Russian Academy of Sciences, 36, Nahimovskiy prospekt, Moscow, 117997, Russia

5 Correspondence to: Alexander G. Ostrovskii (osasha@ocean.ru)

Abstract. The time series of vertical profiles of hydrophysical parameters and dissolved oxygen are critical for identifying trends in water column stratification, mixing and ventilation in the Black Sea. Due to global warming, warm winters have recently become common over the Black Sea, and the temperature in the cold intermediate layer (CIL) is increasing. Regular measurements that are as frequent as every 2 h were performed using a moored profiler near the shelf break at a depth of 220 m in the northeastern Black Sea from January to early March 2016 to assess the temporal dynamics of the oxygen inventory over the upper part of the continental slope on timescales from hours to months. The moored profiler was equipped with a sensor suit that included the CTD 52-MP CTD with the fast oxygen sensor SBE43F and the acoustic Doppler current meter Nortek Aquadopp 2 MHz, which allowed for direct observations of the CIL temperature, the pycnocline structure, the current velocity and the oxygen stratification, in particular, the depths of the hypoxia onset. The average oxygen inventory below a depth of 30 m was 24.9 mol m⁻². Relatively high/low oxygen inventory cases were related to the thin/thick main pycnocline that was associated with the inshore/offshore location of the Black Sea Rim Current. The pycnocline hindered the vertical transport of oxygenated water to the CIL. The new CIL emerged by horizontal advection above the pycnocline only at the end of the observational survey. The vertical displacements of the hypoxia onset depth ranged from 97-170 m, while the shelf edge depth in this region usually ranges from 90-100 m. Intermittently, the hypoxia boundary depth fluctuated on two time scales: ~17 h due to the inertial oscillations and approximately 5 days due to the current meanders and eddies. Further efforts are urgently needed for monitoring the rise of hypoxia onset depth above the shelf break in the Black Sea.

1 Introduction

The Black Sea is a semienclosed sea basin with a very limited water exchange with the Mediterranean Sea; thus, its stratification and circulation are remarkably sensitive to climatic fluctuations and global warming (for example, refer to Stanev et al., 1995, Belokopytov, 2011, Capet et al., 2012, Dorofeev et al., 2013, Dorofeev, Sukhikh, 2016, and Miladinova et al., 2017). The Black Sea is prone to natural hydrogen sulfide contamination, and oxygen-dependent life forms only exist in its top layer, which has a thickness less than 200 m and is most susceptible to atmospheric impacts (Oguz et al., 2003, Capet et al., 2004, Mikaelyan et al., 2013, Capet et al., 2014, Stanev et al., 2014). The stress of the ecosystem is aggravated by the fact that the shelf is narrow, with the exception of the NW part; thus, the benthic habitat is small compared to the total



area of the Black Sea. In general, factors that provide the resistance of the Black Sea ecosystem to anthropogenic and climatic effects are weaker than those in other marginal seas adjacent to the European continent.

In the wintertime, intensive cooling and vertical convective mixing are known to occur in the Black Sea, which enables the top layer to achieve its maximum thickness and minimum temperature (refer to Piotukh et al., 2011 and corresponding references). In summer, a seasonal thermocline is formed above the least heated layer termed as the cold intermediate layer (CIL). This seasonal thermocline blocks vertical turbulent mixing, and to a considerable extent, isolates the CIL from atmospheric forcing. For this reason, the thermohaline properties below the seasonal thermocline retain the “memory” of the wintertime cooling. This memory affects the distribution and bioproductivity of phytoplankton, which is sensitive to density stratification. In addition, the intensity of wintertime convective mixing governs the degree to which the top sea layer is enriched by biogenic substances from its underlying layers, which affects the intensity of the succeeding development of plankton communities (Oguz et al., 2003).

Cooling and convective mixing processes that occur in winter supply oxygen to the top part of the main pycnocline, where turbulence rapidly decays (Gregg, Yakushev, 2005, Zatsepin et al., 2007).

The wintertime measurements of oxygen in Black Sea waters have been very irregular. Gregg and Yakushev (2005) stressed that understanding the origin of the CIL has been hampered by the scarcity of winter observations. Detailed comprehensive studies, including the microstructure measurements and probing in the center of the cyclonic gyre in anomalously cold winter conditions, were completed only in March, 2003 (Gregg, Yakushev, 2005). We assume that they were never repeated. According to the obtained data, freezing air outbreaks drove convection that cooled the surface mixed layer to 6.1°C and deepened it to 40 m, which directly ventilated the upper 80% of the CIL. The concentrations of dissolved oxygen were ~350 $\mu\text{mol L}^{-1}$ in the mixed layer and rapidly decreased to 70 $\mu\text{mol L}^{-1}$ at the base of the CIL, 9 m below the mixed layer. The turbulent fluxes were too weak to reach the suboxic layer (SOL), whose top was 4 m below the bottom of the CIL and well removed from direct surface replenishment (Gregg, Yakushev, 2005).

The vertical exchange processes in the deep sea area and its continental slope region differ in the Black Sea (refer to, e.g., Zatsepin et al., 2003, Stanev et al., 2013) because the total cyclonic circulation is characterized by substantial coastal downwelling and upwelling in the central part of the Black Sea, which leads to the redistribution of the top layer waters (including the CIL water) between the central zone and coastal zone.

Since 2010, the data from ARGO buoys equipped with oxygen sensors became available for the Black Sea. The studies based on these data enabled quantitative assessments of the differences between the vertical structure in the central part of the Black Sea and the vertical structure in its periphery (Stanev et al., 2013). The oxygenated layer in the upper ocean in the central basin was approximately two times thinner than that in the coastal zone, and the temporal variations of its thickness were very small (approximately 20 m). Conversely, the depth of the dissolved oxygen isoline 5 $\mu\text{mol L}^{-1}$, which indicates the oxic-anoxic interface around the continental slope, underwent changes of more than 75 m in only several weeks of the ARGO float travel time. Numerous strong upward bursts of the low oxygen layer that reach 50 m in the deep basin and 75 m in the coastal zone were observed, which manifest the importance of the mesoscale processes (Stanev et al., 2013).



However, the ARGO buoys profiled the water column at five-day intervals. Therefore, their data could not be used to evaluate typical time scales of short-time fluctuations in the oxygen inventory.

The long-term trends assessed with the ARGO buoy data and the old archive data that pertained to marine and laboratory measurements demonstrated that the oxygen inventory had been decreasing in the Black Sea since the second half of the 20th century (Capet et al., 2016). These trends were apparently exacerbated by global warming, which can contribute to the elevation of the hydrogen sulfide boundary.

As stressed in (Friedrich et al., 2014), ship-based monitoring cannot address the temporal dynamics of a low oxygen environment on shorter timescales and episodic low oxygen events. Because the Black Sea ecosystem responses depend on the frequency, duration, and severity of hypoxia events, continuous monitoring of oxygen is required.

The article (Capet et al., 2016) emphasized that the following objectives are important in the present stage of Black Sea research:

- determining the extent that the shoaling of the oxygen penetration layer may entrain the shoaling of the hydrogen sulfide onset depth;
- establishing a system for continuous monitoring of the oxygen inventory and ventilation of the CIL;
- clarifying and quantifying the diapycnic and isopycnic ventilation processes at the periphery of the basin, including mesoscale dynamic structures, and understanding how the intensity of mixing is related to the Rim Current dynamics.

The article (Capet et al., 2016) suggests that these tasks should be approached by using an observation network of moored and drifting profilers equipped with oxygen and hydrogen sulfide sensors. Reasoned by this statement of the problem, we mounted the moored Aqualog profiler equipped with a high-accuracy oxygen sensor (refer to (Ostrovskii and Zatsepin, 2016) for the detailed description of the instrumentation) at the NE Black Sea periphery, namely, in the top part of the continental slope near the Gelendzhik Bay, from January to March 2016.

The mooring site was located near the boundary Rim Current, which encircles the entire Black Sea basin. In this region the ventilation processes in the top layer are much more diversified than those that occur in the open sea. In particular, the Rim Current that meanders and the formation of mesoscale eddies in the NE part (Zatsepin et al. 2003) cause a high amplitude (minimum of 50 meters) and relatively rapid (on the scale of several days) vertical oscillations of the pycnocline and oxycline (Ostrovskii et al. 2010, Zatsepin et al. 2013). The Rim Current interaction with the bottom relief creates near-bottom Ekman currents and water flows in the direction normal to the edge of the continental shelf (Ostrovskii and Zatsepin, 2016, Elkin et al., 2017). Wind induced upwellings although they are not frequent in the NE zone (Zatsepin et al., 2016) initiate locally a short-time redistribution of the oxygen concentration in the shelf and slope waters of the Black Sea.

Due to the high short-term variability at the NE Black Sea periphery, the temporal scales of the oxygen inventory fluctuations and the oxygen redistribution over depth in these fluctuations must be described more thoroughly, typical vertical distributions of oxygen concentration must be identified, the observed vertical distributions must be explained, and any gaps in our understanding of the effect of oxygen fluctuations on the sea ecosystem must be identified. These tasks can only be solved by analyzing the time series of vertical profiles for both hydrophysical and hydrochemical parameters. The



time resolution of the measured data must be sufficiently high to address any transient processes that may have a long-term effect on the ecosystem (Jessen et al., 2017). These data were not available to Black Sea oceanographers until recently.

This paper considers these issues by analyzing a unique data set that describes the vertical profiles of oxygen content, temperature and salinity of water, and speed and direction of currents, as well as acoustic backscattering on suspended matter. These profiles were obtained in winter, when the maximum amount of oxygen inventory in water is achieved, by frequent cycling of the Aqualog profiler between the near-surface sea layer and the near-bottom layer below the hydrogen sulfide boundary.

This paper is organized rather plainly: the observational methods are presented in Sections 2, data processing results and a discussion are provided in Sections 3 and 4, conclusions are brought into Section 5.

10 2 Measurement methods

The oxygen inventory measurements were taken on the moored buoy station at 44°32.372'N 37°54.868'E near Gelendzhik Bay in the NE Black Sea (Fig. 1). The shelf is normally shallow, less than 100 m deep with a maximum width of 4 km in this region. The mooring was deployed at approximately 220 m and operated from January 1 to March 6, 2016.

The mooring was equipped with the Aqualog profiler (Ostrovsky et al., 2013) and featured an SBE 52-MP CTD temperature, conductivity and pressure probe with a SBE43F fast oxygen sensor and an acoustic Doppler current meter Nortek Aquadopp 2 MHz. The equipment set was described in (Ostrovskii, Zatsepin, 2016).

The Aqualog was programmed for profiling every 2 hours to obtain 24 depth profiles of seawater parameters each day. The parking depth of the profiler was 205 m, and the upper profiling depth was 25 m. Each profiling cycle was started at an exact UTC hour from the parking depth. After ascending to the upper depth limit in approximately 14 min, the profiler would stop for 20 min and then descend for approximately 13 min.

Several profiler faults occurred at the beginning of the observations, which resulted in data loss for a total of four days. Starting January 9, the profiler smoothly worked until it was recovered after taking approximately 1490 multiparameter profiles.

Soon after recovery, the SBE 52-MP CTD probe with the SBE43F sensor was sent to the manufacturer for calibration. All sensors were in very good condition and demonstrated the smallest possible drift. The modified calibration coefficients were considered during the processing of the measurement data.

The data employed in our studies of currents comprised the data obtained during the ascent of the profiler. The Aquadopp acoustic current meter was mounted in the top part of the apparatus, and the current measurements in the ascending sections were taken in undisturbed waters.

The CTD and dissolved oxygen data were obtained every 2 s. The current meter sampling frequency was 4 Hz. To suppress the measurement noise, the current meter data were smoothed by the running mean using a fixed window length of 51 samples, which corresponds to a vertical scale of approximately 2.5 m.



To assess the conditions that are favorable for developing turbulent mixing, the estimates of the Richardson number Ri are applied. The linear theory predicts the development of the shear instability of stratified fluid when Ri is less than the critical value, which is equal to $Ri = 0.25$. The value $Ri < 1$ indicates the possibility of flow instability (Orlanski and Bryan 1969).

5 The gradient Richardson number was computed as follows:

$$Ri = N^2 / |\Delta U / \Delta z|^2 \quad (1)$$

where $N^2 = g / \rho_0 (\Delta \sigma_\theta / \Delta z)$ is the Brunt–Väisälä frequency, $\Delta \sigma_\theta$ and ΔU denote the difference in the water density and the
 10 difference in the horizontal current velocity, respectively, between adjacent depth bins with the thickness $\Delta z = 4$ m.

3 Results

Direct measurements showed that the vertical distribution of oxygen underwent significant fluctuations in January–March 2016 (Fig. 2). The fluctuations of 3–7 days were observed mainly in the layer deeper than $\sigma_\theta = 14$ kg m^{−3} isopycnal. In the second half of January and in the first half of February, these fluctuations were slightly modulated by near-inertial
 15 oscillations with a period of about 17 hours. Noticeably the temporal variations of the dissolved oxygen were usually locked to the vertical displacements of the isopycnal surfaces. The upper layer of the sea above isopycnal $\sigma_\theta = 14$ kg m^{−3} was usually well mixed. There was a seasonal trend of the dissolved oxygen from 280 to 310 μmol L^{−1} in the upper mixed layer.

The fluctuations of dissolved oxygen content and water density were correlated with the current velocity. Basically, the temporal variability of the flow could be described as that due to a meandering near-coastal jet and propagating
 20 mesoscale and submesoscale eddies. Notice that the profiler mooring was located in the Rim Current zone on the periphery of the basin-wide cyclonic gyre, where the flow of the NW direction prevailed. The events of strengthening of the NW transport persisted for up to 7 days with the current speed occasionally reaching 45 cm/s in the upper layer of the sea (Fig. 3). At times, the near-inertial motions emerged and the relevant reversals in the direction of the flow velocity could be observed, such as from 16 to 25 of January.

25 The cross-shelf component of the flow velocity was much weaker than that directed along the shelf (Fig. 3). The flows towards the deep basin were intermittent and rather weak in the upper layer of the sea. During the survey, there were no upwelling events that would lead to a significant increase in water exchange between the sea shelf zone and the deep sea.

Sometimes over the mooring site in the upper layer of the sea, the SE flow appeared for 1–2 days, but its speed did not exceed 20 cm/s. In such cases, apparently, the station was on the eastern periphery of the anticyclonic vortices, where the
 30 orbital velocity was southeastward. During the second half of the survey, the southeastward transport was observed more often. The SE current was noticeable in the pycnocline between isopycnals σ_θ from 14.5 to 16 kg m^{−3}.



From January to March 2016, the average oxygen inventory I in the region of the Aqualog station in the sea below 30 m was $\bar{I}_{30} = 24.9 \text{ mol m}^{-2}$. The value of I highly fluctuated on two scales: near-inertial scale and of three to five days (refer to Fig. 4). The standard deviation of the I_{30} time series was 3.5 mol m^{-2} .

To evaluate the total average oxygen inventory estimate one may assume that the average oxygen content in the 30 m thick near-surface sea layer may be equal to the value $[\text{O}_2] = 270 \div 300 \text{ } \mu\text{mol L}^{-1}$ observed at a depth of 30 m, where the instrumental measurements with the Aqualog profiler were obtained. Then the total average oxygen inventory for the entire water column would be the value \bar{I}_{30} increased by approximately $8 \div 9 \text{ mol m}^{-2}$ as follows $\bar{I}_{total} = 33 \div 34 \text{ mol m}^{-2}$.

The oxygen inventory distribution with depth substantially varied with time. In particular, the distribution was extremely small ($I_{\sigma_{14}} \leq 3.5 \text{ mol m}^{-2}$) for approximately 10% of all profiles in the layer below the $\sigma_{\theta} = 14 \text{ kg m}^{-3}$ isopycnal (Fig. 4). In these cases, the oxygen-rich and deep upper layer was separated by a narrow oxycline from the underlying waters that were subjected to the lower oxygen content conditions (Fig. 5). The thermohaline stratification was characterized by a very sharp pycnocline (Fig. 6): the sample-averaged Brunt–Väisälä frequency in the region of the maximum density gradient amounted to $\langle N \rangle = 0.041 \text{ s}^{-1}$ with the median value $\text{med}(N)$ equal to 0.037 s^{-1} . The average vertical distribution of the oxygen inventory for $I_{\sigma_{14}} \leq 3.5 \text{ mol m}^{-2}$ had a two-layered structure and a single-step profile (Fig. 7); the oxygen content decreased from approximately 280 to $10 \text{ } \mu\text{mol L}^{-1}$ across the oxycline with a maximum thickness of 40 m. Note that in mid-January 2016, the distance between the oxygen-rich zone and the upper boundary of the suboxic zone, where $[\text{O}_2] < 10 \text{ } \mu\text{mol L}^{-1}$, was sometimes less than 20 m.

In 89% of the cases, the oxygen slowly decreased with the depth in the oxycline of a typical thickness $\sim 100 \text{ m}$ (Fig. 7). In the second half of February, the thickness of the oxycline began to increase, and the oxygen inventory in the sea below 30 m decreased from its peak values $I_{30} = 30 \div 35 \text{ mol m}^{-2}$ beginning late January or early February to $I_{30} = 21 \div 25 \text{ mol m}^{-2}$ in early March (Fig. 4).

As the seasonal changes evolved, the depths of hypoxia onset, SOL, CIL and pycnocline fluctuated with large amplitudes with a period of the near-inertial oscillation (Fig. 8). The onset of hypoxia was defined as follows: $[\text{O}_2] = 63 \text{ } \mu\text{mol L}^{-1}$. This criterion for hypoxia conditions was introduced in (Middelburg, Levin, 2009) and employed for the Black Sea Crimean shelf data (Jessen et al., 2017) as a threshold value, where the low oxygen content in water starts affecting the fauna, the structure of animal communities, and functions of the marine ecosystem.

Intermittently, the depth of hypoxia onset fluctuated with an amplitude of $\sim 50 \text{ m}$. These fluctuations can last 3–7 days interleaved by quiet periods of several days. They were observed in the layer of 100–150 m, i.e., too deep to be directly associated with the storms on the sea surface. The atmospheric effects in this layer may be indirectly traced to meandering and temporary intensification of the Rim Current or propagation of inertia-gravity wave packets from the deep basin.

According to our data, the onset of hypoxia often appeared in the region of maximum density gradients in the pycnocline and occurred above the depth of the minimum temperature in the CIL until March 3. The CIL gradually eroded while remaining to be unventilated all winter in this region. The temperature increased from 8.45 in early January to 8.6°C in late February and as late as the beginning of March, when a new CIL emerged as a result of horizontal advection in the layer



40 m above the old CIL (Fig. 9). In this new CIL, the temperature of 8.35°C was recorded: the absolute minimum temperature for the entire duration of our observations. The new CIL was located above the hypoxia zone.

4 Discussion

Few studies of the oxygen distribution in the Black Sea periphery have mentioned short-term oxygen content fluctuations in the top sea layer that extends to the top boundary of the main pycnocline. The observations using drifting ARGO buoys provided insight into the important role of mesoscale processes both in the central part of the basin and the Rim Current zone (Stanev et al., 2013). However, quantitative data on the short-term variability of the hypoxia layer depth and the suboxic zone depth is lacking. Mesoscale and submesoscale eddies, subsurface waves and upwelling events were known to interact in the shelf and slope zone at time scales less than 10 days (Zatsepin et al., 2013).

The results obtained in this study highlight basic time scales of the oxygen inventory changes in the NE Black Sea: the inertial period, and the scale of approximately five days. The short term variations are superimposed on the seasonal cycle. The maximum total oxygen inventory can be as large as 42÷43 mol m⁻² in February 2016 with the winter average of 33÷34 mol m⁻². The latter value shows agreement with the annual average for this region (refer to Fig. 4 in (Capet et al., 2016)).

What were the hydrophysical conditions when both the pycnocline and the oxycline became so thin in wintertime? Based on our data, these conditions can be described by strong NW currents (Fig. 10) in the top layer above the pycnocline. The maximum speed of the NW current sometimes exceeded 0.4 m/s. The boost of the current speed may occur when the Rim Current axis shifts toward the shelf in the region. When the Rim Current is pressed against the continental slope, the isopycnals are usually lowered by 40-60 m (Zatsepin et al., 2011).

A countercurrent of the SE direction was observed in the narrow pycnocline. Its maximum speed (sometimes as high as 0.3 m/s) was in the layer where the vertical density gradient attained its maximum values. This countercurrent was observed in 2007 during an experiment with a moored profiler in the Black Sea (Ostrovskii et al., 2010).

While the oxygen inventory was limited in the layer of $I_{\sigma 14} < 3.5$ mol m⁻² in the region of the mooring station, the vertical oxygen distribution in the top layer was uniform, and the stratification was almost neutral. The median of the Richardson numbers med(*Ri*) (Fig. 11) calculated by binning the data for each profile at 4-meter layers indicated that the condition $Ri < 0.25$ required for vertical turbulent mixing may often develop in the top layer of 100 m.

In the pycnocline, the median values of *Ri* abruptly increased to 2÷6. Under the pycnocline (down to the 200 m depth), conditions for turbulent mixing at the vertical scale of 4 m usually do not occur considering the estimated *Ri* values. But we cannot exclude that they do occur at smaller vertical scales.

The presence of a well-mixed deep top layer is confirmed by the data on the distribution of acoustic backscatter, which was measured by the acoustic Doppler current meter Nortek operated at 2 MHz. According to the estimated cross-correlation amplitudes of acoustic backscatter (not shown here), the suspended matter coherently fluctuated throughout the entire top layer. Under the pycnocline, the suspended matter slowly subsided at an average rate of 3.5 mm/s.



As mentioned in the Introduction, the dynamic processes in the Rim Current zone, which is predominantly localized near the continental slope, differ from the conditions in a dynamically less active deep sea basin of the Black Sea. In the continental slope area in the NE part of the Black Sea during the very cold winter, the convection may penetrate to a depth of 120-130 m (Ostrovskii, Zatsepin, 2016).

5 In the center of the western cyclonic gyre, the depth of the top mixed layer was limited by 40 m also in an anomalously cold winter (Gregg, Yakushev, 2005). The concentrations of dissolved oxygen in the mixed layer were $350 \mu\text{mol L}^{-1}$. The remaining thin stratified part of the CIL was cooled by turbulence accompanying the cold wind outbreak. The bottom of the CIL was approximately located at the same depth ~ 50 m as the onset of hypoxia (Gregg, Yakushev, 2005).

10 Short-term fluctuations of the onset of hypoxia in the deep basin do not seriously endanger the ecosystem because the plankton coherently fluctuates over the depth with the isopycnic surfaces and the oxygen isolines almost always move in accordance with the isopycnals.

15 However, the pycnocline shrinkage to a thickness of 15-20 m near the shelf edge for several hours may create favorable conditions for entraining biota into the suboxic zone when an internal wave breaks near the bottom of the sea. This wave breaking is common when the vertical shift of speed considerably increases after the internal wave runs onto the continental slope or shelf. In the NE Black Sea, the maximum amplitude of short-term (7-8 minutes) subsurface waves on the shelf may be as high as 16 m (Bondur et al., 2018 (to be published)). In the NW Black Sea, intensive subsurface waves in the lower part of the pycnocline in the halocline were primarily observed in the continental slope area in autumn, winter and summer (Morozov et al., 2017). During these measurements in the main pycnocline in December 2012, vertical current profiles of the large internal waves with a vertical length of 50-60 m were observed.

20 An abruptly fluctuating onset of hypoxia in the shelf and slope sea zone may considerably affect the benthos. Note that the shelf edge in the NE Black Sea predominantly occurs in the depth range of 90-100 m; thus, the extensive shoaling in the hypoxia onset depth should cause penetration of low oxygen water into the outer shelf. The hypoxia events near the shelf edge can be observed based on our data for January 1-3, 2016. Ground species living at the top part of the continental slope adapt to fluctuations of the oxygen because these species should experience the hypoxia conditions at regular intervals of
25 ~ 17 hours.

5 Concluding remarks

30 A higher total content of oxygen that exceeds 34 mol m^{-2} and sometimes 40 mol m^{-2} in the NE Black Sea slope water column was observed in approximately 11% of the profiles collected during a warm winter in January to early March 2016. An oxygen inventory increases when the Rim Current axis is shifted closer to the shelf edge. In these conditions, the top mixed layer is deep (110-130 m) and oxygen-rich ($270\text{-}300 \mu\text{mol L}^{-1}$ of oxygen on the average), whereas both the thickness of pycnocline and the oxycline decrease to approximately less than 40 m.



Weakening of the Rim Current jet or its shift toward the open sea causes an expansion of the pycnocline, and as a consequence, a decrease in the total oxygen inventory (less than 33 mol m^{-2}). In the latter case, stable stratification in the thick pycnocline tends to suppress vertical turbulent mixing from a depth of 30–40 m.

The Rim Current that flows in the NW direction occupies the upper sea layer to the top of the pycnocline. The vertical shear of the current speed in the lower part of the current is too small to overcome stable stratification in the pycnocline, and therefore, disables turbulent mixing to reach the CIL. In the conditions of a relatively warm winter, the maximum gradient in the pycnocline is located above the CIL core; thus, the CIL cannot be ventilated more or less intensively. By the end of the warm winter, a new CIL may be formed due to horizontal advection of water above the old CIL. Water in this new CIL is rather warm ($8.3\div 8.4^\circ\text{C}$) but may be oxygen-rich ($[\text{O}_2] = 240\text{--}270 \mu\text{mol L}^{-1}$). Considering that the new CIL is located above the hypoxia zone, essential changes in plankton migrations may occur.

In the wintertime, when the top layer of the Black Sea is intensively ventilated, the depth of the hypoxia onset may be as shallow as 97 m near the boundary of the sea shelf and the continental slope, i.e., almost above the shelf edge in the study area. Probably the life cycles of the near-bottom-layer species that live at the outer shelf deeper than ~95 m had to adapt to significant fluctuations of oxygen contents in the water at time scales of approximately 17 hours and ~5 days. Studies of the biota in the boundary area of the Black Sea ecosystem are underway (Jessen et al., 2017).

A key question is how the oxygen stratification will change in the conditions of continued global warming. Will the climatic change cause the $63 \mu\text{mol L}^{-1}$ hypoxia zone to persist above the sea shelf edge and cause the benthos at the NE Black Sea shelf to enter hibernation associated with the low oxygen content in the near-bottom layer? In the worst case, the broad shelf region south of the Kerch Strait with its fishing grounds in just 100 km to the north-west of our observational site would become the next environmental risk area.

Acknowledgements. Authors are thankful to P.A. Stunzhas for discussions about measurements of the dissolved oxygen in the Black Sea. This research was performed in the framework of Program of the Presidium of Russian Academy of Sciences No. 1-2-50 (0149-2018-0022) and supported in part by Russian Fund for Basic Research (project No. 17-05-00381).

References

- Belokopytov, V.: Interannual variations of the renewal of waters of the cold intermediate layer in the black sea for the last decades, *Phys. Oceanogr.*, 20, 347–355, doi:10.1007/s11110-011-9090-x, 2011.
- Bondur, V. G., Serebryany, A. N., and Zamshin, V. V., 2018. Anomalous train of internal waves of record heights on the shelf of the Black Sea, generated by the atmospheric front, *Doklady Earth Sciences*. (in press).
- Capet, A., Barth A., Beckers, J.-M., and Grégoire, M.: Interannual variability of Black Sea's hydrodynamics and connection to atmospheric patterns. *Deep Sea Research Part II: Topical Studies in Oceanography*, 77–80, 128–142, doi:10.1016/j.dsr2.2012.04.010, 2012.



- Capet, A., Stanev, E. V., Beckers, J.-M., Murray, J. W., and Grégoire, M.: Decline of the Black Sea oxygen inventory, *Biogeosciences*, 13, 1287–1297, doi:10.5194/bg-13-1287-2016, 2016.
- Dorofeev, V. L., and Sukhikh, L. I.: Analysis of variability of the Black Sea hydrophysical fields in 1993–2012 based on the reanalysis results, *Phys. Oceanogr.*, 1, 33–47, doi: 10.22449/1573-160X-2016-1-33-47, 2016.
- 5 Dorofeev, V. L., Korotaev, G. K., and Sukhikh, L. I.: Study of long-term variations in the Black Sea fields using an interdisciplinary physical and biogeochemical model, *Izvestiya Atmos. Oceanic Phys.*, 49, 622–631, doi:10.1134/S0001433813060054. 2013.
- Elkin, D. N., Zatsepin, A. G., Podymov, O. I., and Ostrovskii, A. G.: Sinking of less dense water in the bottom Ekman layer formed by a coastal downwelling current over a sloping bottom, *Oceanology*, 57, 478–484, doi:10.1134/S0001437017040051, 2017.
- 10 Friedrich, J., Janssen, F., Aleynik, D., Bange, H.W., Boltacheva, N., Çagatay, M. N., Dale, A. W., Etiope, G., Erdem, Z., Geraga, M., Gilli, A., Gomoiu, M. T., Hall, P. O. J., Hansson, D., He, Y., Holtappels, M., Kirf, M. K., Kononets, M., Konovalov, S., Lichtschlag, A., Livingstone, D. M., Marinaro, G., Mazlumyan, S., Naeher, S., North, R. P., Papatheodorou, G., Pfannkuche, O., Prien, R., Rehder, G., Schubert, C. J., Soltwedel, T., Sommer, S., Stahl, H., Stanev, E. V., Teaca, A.,
- 15 Tengberg, A., Waldmann, C., Wehrli, B., and Wenzhöfer, F.: Investigating hypoxia in aquatic environments: diverse approaches to addressing a complex phenomenon, *Biogeosciences*, 11, 1215–1259, doi:10.5194/bg-11-1215-2014, 2014.
- Gregg, M. C., and Yakushev, E.: Surface ventilation of the Black Sea Cold Intermediate Layer, *Geophys. Res. Lett.*, 32, 1–4, doi:10.1029/2004GL021580, 2005.
- Jessen G. L., Lichtschlag, A., Ramette, A., Pantoja, S., Rossel, P. E., Schubert, C. J., Struck, U., and Boetius, A.: Hypoxia causes preservation of labile organic matter and changes seafloor microbial community composition (Black Sea), *Sci. Adv.*, 3(2):e1601897, doi:10.1126/sciadv.1601897, 2017.
- 20 Mikaelyan, A. S., Zatsepin, A. G., and Chasovnikov, V. K.: Long-term changes in nutrient supply of phytoplankton growth in the Black Sea, *J. Mar. Syst.*, 117–118, 53–64, doi:10.1016/j.jmarsys.2013.02.012, 2013.
- Miladinova, S., Stips, A., Garcia-Goriz, E., and Macias Moy, D.: Black Sea thermohaline properties: Long-term trends and variations, *J. Geophys. Res. Oceans*, 122, 5624–5644, doi:10.1002/2016JC012644, 2017.
- 25 Morozov A. N., Lemesko, E.M., Shutov, S. A., Zima, V. V., and Deryushkin, D.V.: Structure of the Black Sea Currents Based on the Results of the LADCP Observations in 2004–2014, *Physical Oceanography*, 1, 25–40, doi:10.22449/1573-160X-2017-1-25-40, 2017.
- Oguz, T., Cokacar, T., Malanotte-Rizzoli, P., and Duclov, H. W.: Climatic warming and accompanying changes in the ecological regime of the Black Sea during 1990s, *Glob. Biogeochem. Cycles*, 17, 1088, doi:10.1029/2003GB002031, 2003.
- 30 Orlanski, I., and Bryan, K.: Formation of the thermocline step structure by large amplitude internal gravity waves, *J. Geophys. Res.*, 74, 6975–6983, 1969



- Ostrovskii, A. G., and Zatsepin, A. G.: Short-term hydrophysical and biological variability over the northeastern Black Sea continental slope as inferred from multiparametric tethered profiler surveys, *Ocean Dynamics*, 61, 797-806, doi:10.1007/s10236-011-0400-0, 2011.
- Ostrovskii, A. G., and Zatsepin, A. G.: Intense ventilation of the Black Sea pycnocline due to vertical turbulent exchange in the Rim Current area, *Deep-Sea Research I*, 116, 1–13, doi:10.1016/j.dsr.2016.07.011, 2016.
- Ostrovskii, A. G., Zatsepin, A. G., Shvoev, D. A., and Soloviev, V. A.: Underwater anchored profiler Aqualog for ocean environmental monitoring, in: Daniels, J.A. (Ed.), *Advances in Environmental Research.*, Nova Science, New York, 179-196, 2010
- Ostrovskii, A. G., Zatsepin, A. G., Soloviev, V. A., Tsibulsky, A. L., and Shvoev, D. A.: Autonomous system for vertical profiling of the marine environment at a moored station, *Oceanology*, 53, 233–242, doi:10.1134/S0001437013020124, 2013.
- Piotukh, V., Zatsepin, A. G., Kazmin, A., and Yakubenko, V.: Impact of the winter cooling on the variability of the thermohaline characteristics of the active layer in the Black Sea, *Oceanology*, 51, 221–230, doi:10.1134/S0001437011020123, 2011.
- Stanev, E. V., He, Y., Grayek, S., and Boetius, A.: Oxygen dynamics in the Black Sea as seen by Argo profiling floats, *Geophys. Res. Letters*, 40, 3085–3090, doi:10.1002/grl.50606, 2013.
- Stanev, E. V., Staneva, J., Bullister, J. L., and Murray, J. W.: Ventilation of the Black Sea pycnocline. Parameterization of convection, numerical simulations and validations against observed chlorofluorocarbon data, *Deep Sea Res., Part I*, 51, 2137–2169, doi:10.1016/j.dsr.2004.07.018, 2004.
- Stanev, E. V., He, Y., Staneva, J., and Yakushev, E.: Mixing in the Black Sea detected from the temporal and spatial variability of oxygen and sulfide – Argo float observations and numerical modelling, *Biogeosciences*, 11, 5707–5732, doi:10.5194/bg-11-5707-2014, 2014.
- Zatsepin, A. G., Ginzburg, A. I., Kostianoy, A. G., Kremenetskiy, V. V., Krivosheya, V. G., Poulain P. M., Stanichny, S. V.: Observation of Black Sea mesoscale eddies and associated horizontal mixing. *J. Geophys. Res.*, V.108, C8. 1-27, doi:10.1029/2002JC001390, 2003.
- Zatsepin, A., Golenko, N., Korzh, A., Kremenetskii, V., Paka, V., Poyarkov, S., and Stunzhas, P.: Influence of the dynamics of currents on the hydrophysical structure of the waters and the vertical exchange in the active layer of the Black Sea, *Oceanology*, 47, 301–312, doi: 10.1134/S0001437007030022, 2007.
- Zatsepin A. G., Ostrovskii, A. G., Kremenetskiy, V. V., Piotukh, V. B., Kuklev, S. B., Moskalenko, L. V., Podymov, O. I., Baranov, V. I., Korzh, A. O., and Stanichny, S. V.: On the nature of short period oscillations of the main Black Sea pycnocline, submesoscale eddies, and response of the marine environment to the catastrophic shower of 2012, *Izvestiya, Atmos. Oceanic Phys.*, 49, 659–673, doi:10.1134/S0001433813060145, 2013.
- Zatsepin, A. G., Silvestrova, K.P., Kuklev, S. B., Piotoukh, V. B., and Podymov, O.I.: Observations of a cycle of intense coastal upwelling and downwelling at the research site of the Shirshov Institute of Oceanology in the Black Sea, *Oceanology*, 56, 188-199, doi:10.1134/S000143701602021, 2016.

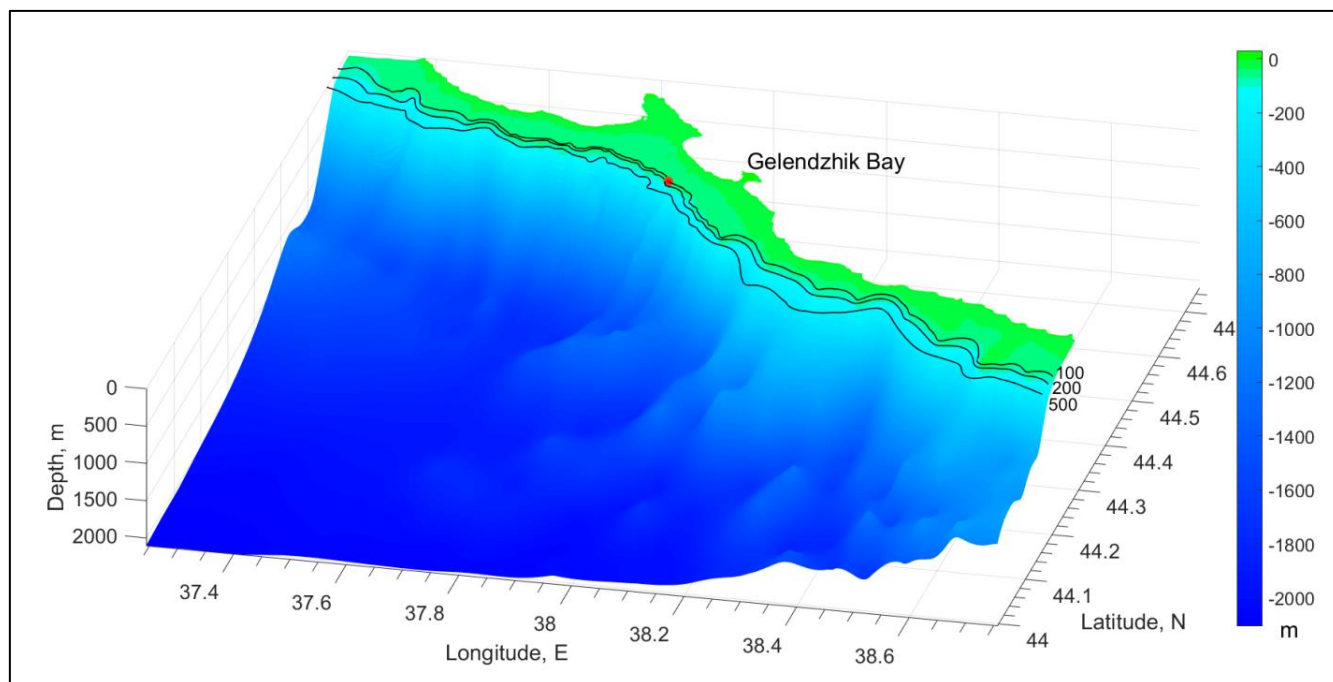


Figure 1: Bottom topography in the NE Black Sea (based on European Marine Observation and Data Network bathymetry; <http://www.emodnet-hydrography.eu/>). Red mark indicates location of the Aqualog profiler mooring. Notice the narrow (width of only a few kilometers) and shallow (depth less than 100 m) sea shelf.

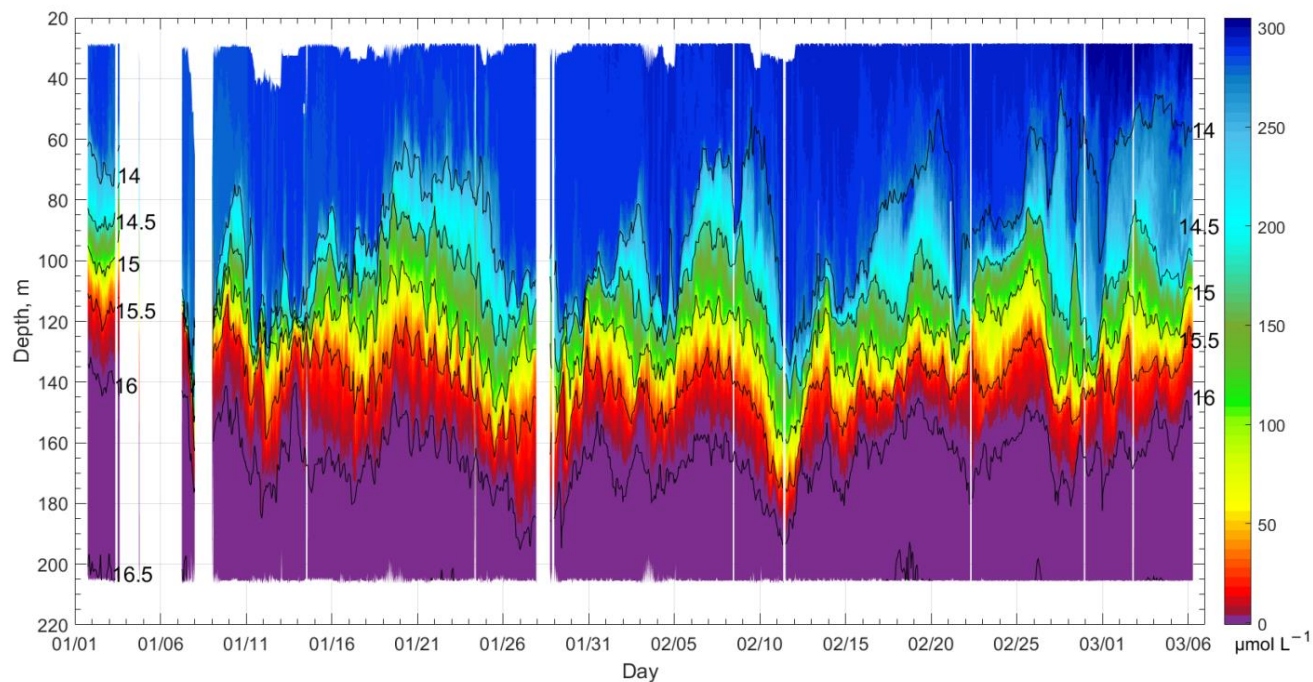


Figure 2: Temporal evolution of the vertical distribution of the dissolved oxygen. The measurements were carried out by using a SBE 43F sensor housed in an Aqualog moored profiler in the NE Black Sea (see Figure 1 for location). The black lines indicate isopycnals σ_θ .

5

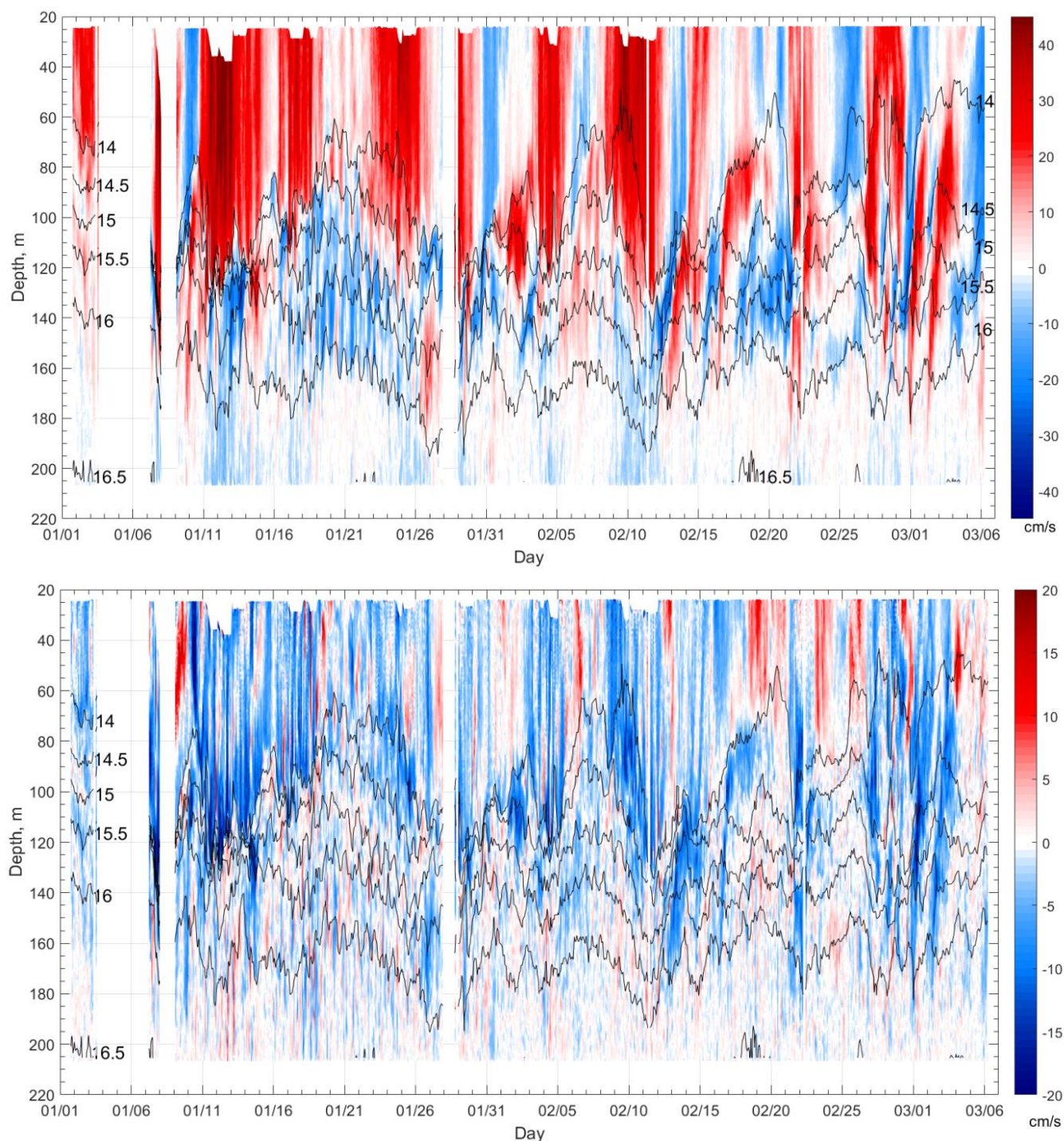


Figure 3: Profiles of along-shore (upper panel) and cross-shore components of the current velocity (lower panel), depicted as colored contours. The isopycnals σ_θ are superimposed (black lines). Note the positive direction of the along-shore axis is 50° , and the positive direction of the cross-shore axis is 310° .

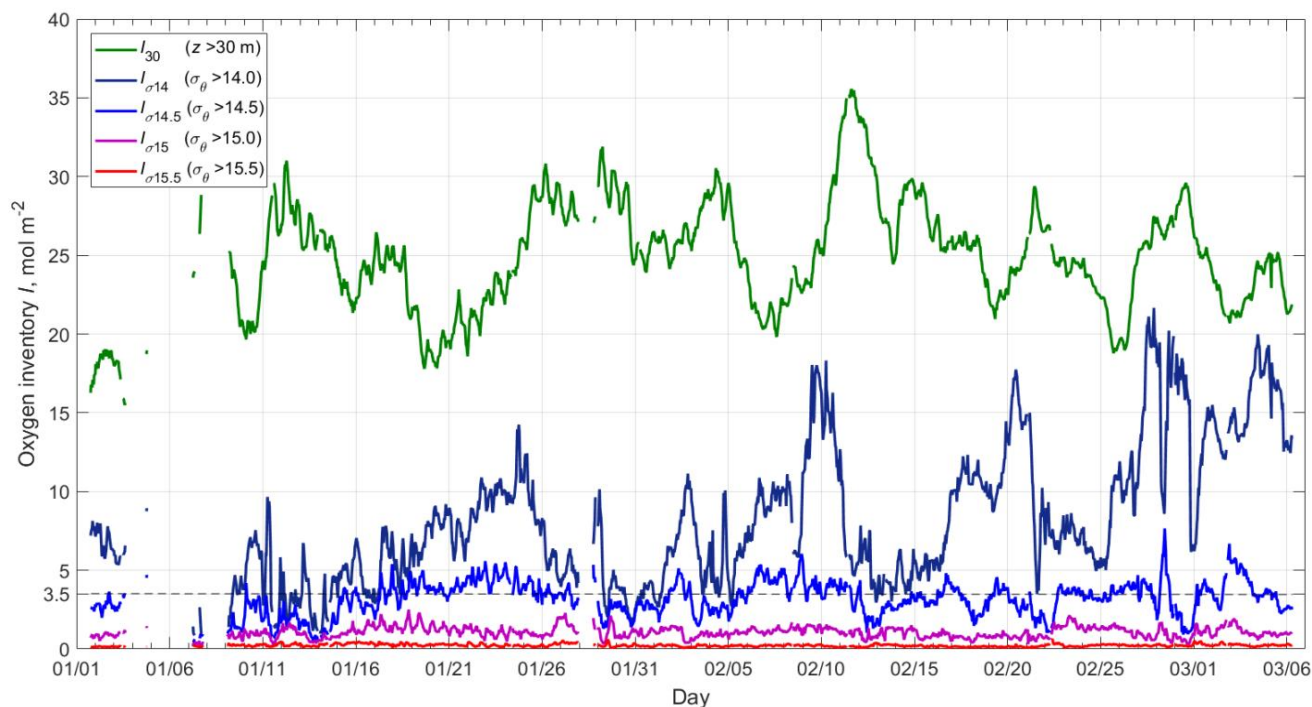


Figure 4: The oxygen inventory I per the Aqualog profiler data taken from January to March 2016. The green line is the oxygen inventory I_{30} in the sea below 30 m. Other colored lines denote the oxygen inventories $I_{\sigma_{14}}, \dots, \sigma_{15.5}$ in the layers below the respective isopycnal depths, as specified in the top left corner of the figure.

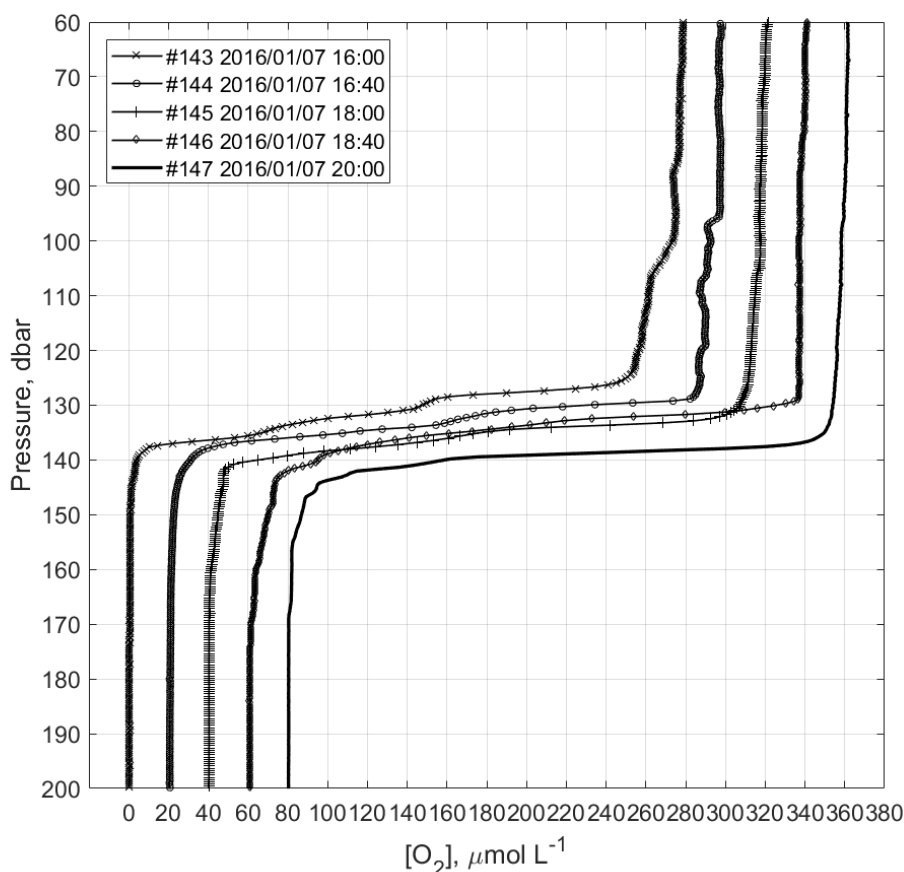


Figure 5: Example series of five profiles $[O_2]^j(z)$, where z is the depth and j is the profile number, $j = 143, \dots, 147$, when the oxygen inventory below the $\sigma_\theta = 14 \text{ kg m}^{-3}$ isopycnal was extremely low $I_{\sigma 14} \leq 3.5 \text{ mol m}^{-2}$. The profile numbers, dates and times are shown in the top left corner. The profiles are separately shifted to the right by $20 \mu\text{mol L}^{-1}$ along the horizontal axis. The odd-numbered profiles were taken when the profiling probe was moving up, and the even-numbered profiles were taken when the profiling probe was moving down. Due to the time-lag of the oxygen sensor, a profile obtained during the descent has slightly different curvatures compared with that obtained during the ascent, particularly at the upper and lower boundaries of the oxycline.

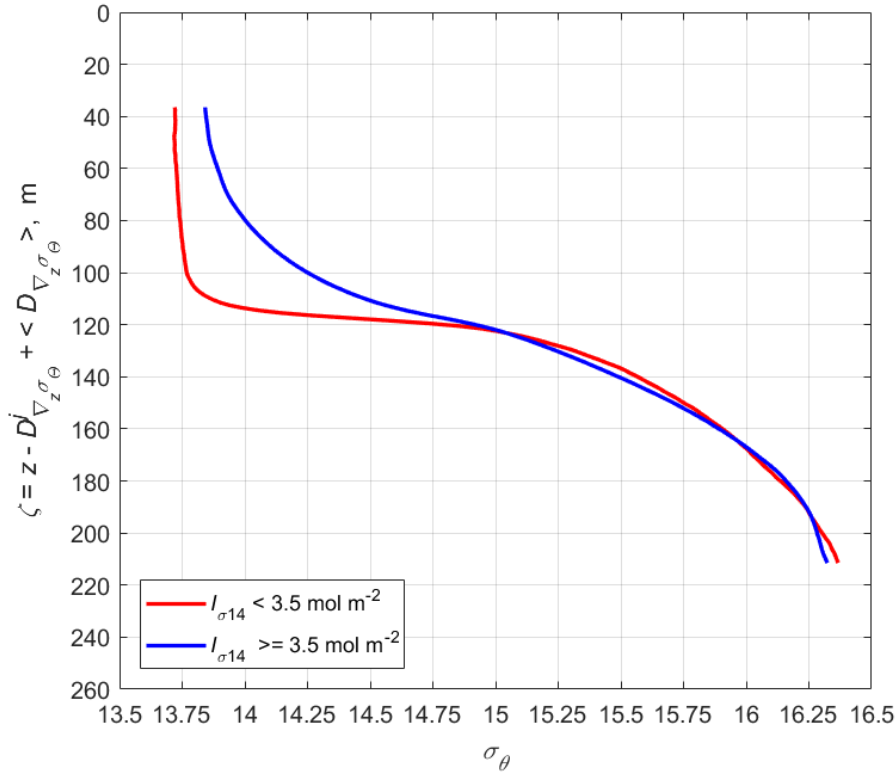


Figure 6: Mean vertical profiles of potential density versus distance from the depth of the maximum density gradient in the pycnocline. The mean values were calculated for an ensemble that consists of M individual profiles $\sigma_\theta^j(z)$, where z is the depth and $j = 1, \dots, M$; each are vertically displaced from the depth of the maximum density gradient in the pycnocline $D_{\nabla_z \sigma_\theta}^j$: $\zeta = z - D_{\nabla_z \sigma_\theta}^j + \langle D_{\nabla_z \sigma_\theta} \rangle$, where $\nabla_z \sigma_\theta = \Delta \sigma_\theta / \Delta z$ and the angle brackets denote the time average. The red curve represents the mean profile for the cases where $I_{\sigma 14} < 3.5 \text{ mol m}^{-2}$. The number of profiles in this ensemble was $M = 145$, i.e., 11% of all profiles. The blue curve is the mean profile for the cases where $I_{\sigma 14} \geq 3.5 \text{ mol m}^{-2}$ ($M = 1248$, 89% of the data).

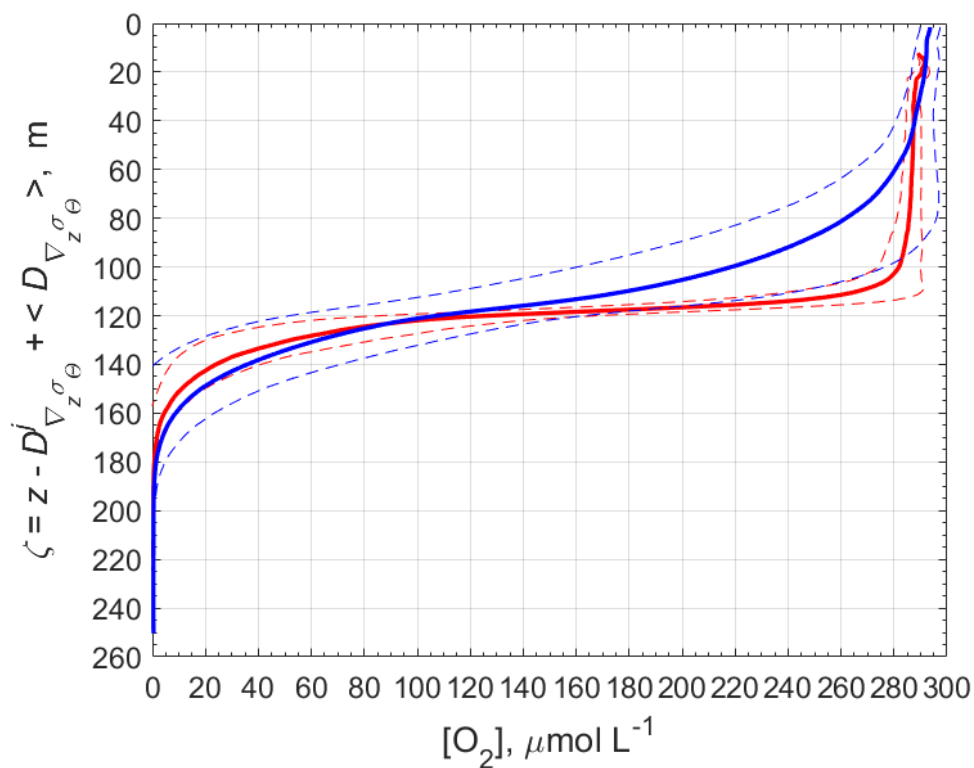


Figure 7: Mean profiles of dissolved oxygen content for $I_{\sigma_{14}} < 3.5 \text{ mol m}^{-2}$ (red curve) and $I_{\sigma_{14}} \geq 3.5 \text{ mol m}^{-2}$ (blue curve).

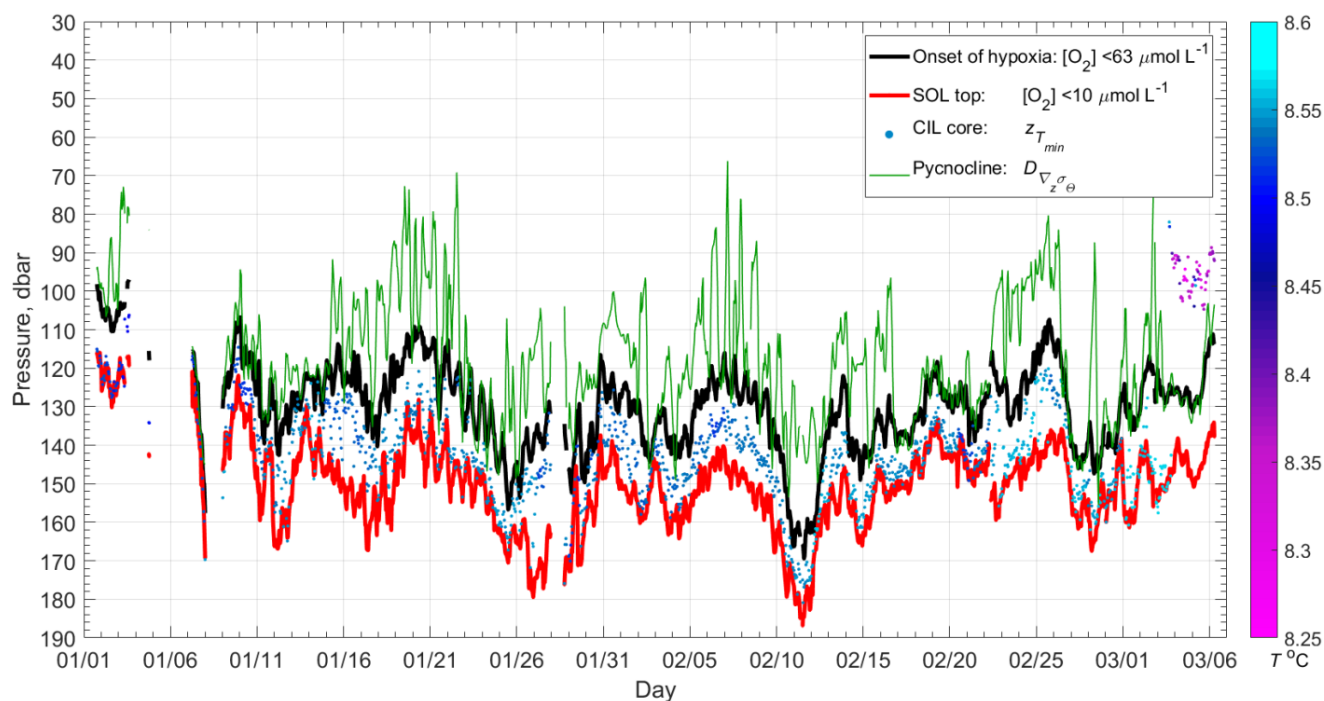


Figure 8: Depths below the onset of hypoxia $[O_2] < 63 \mu\text{mol L}^{-1}$, the suboxic layer $[O_2] < 10 \mu\text{mol L}^{-1}$, the regions of maximum vertical gradient of density and minimum water temperature (regarding the colored spots, refer to the color scale to the right of the figure).

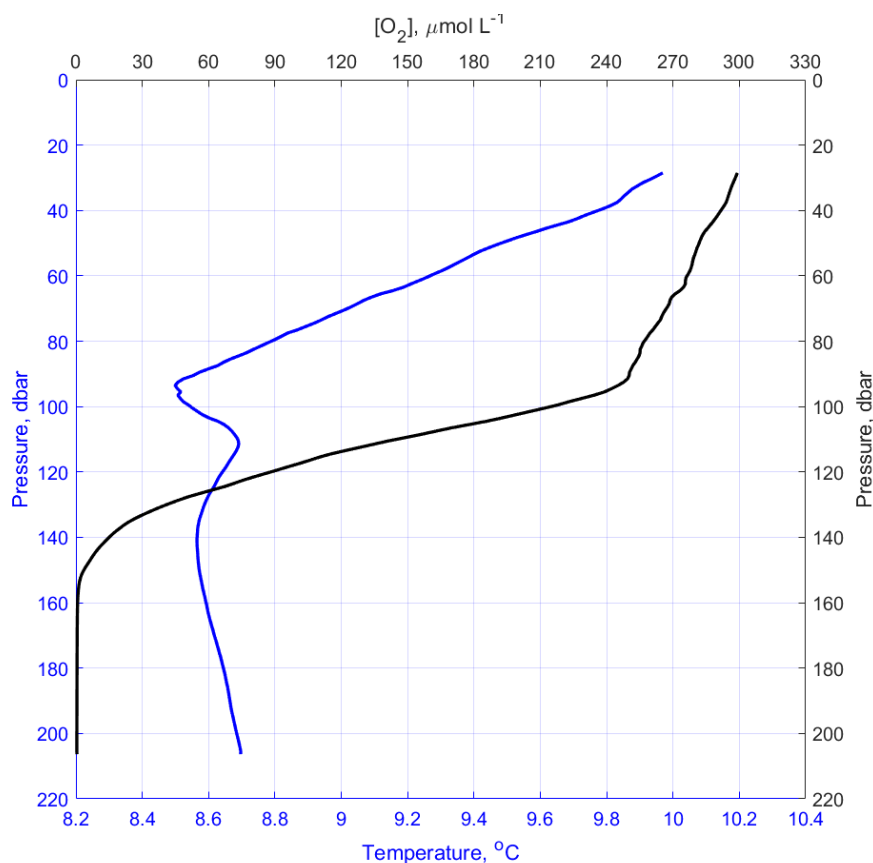


Figure 9: Mean profiles of water temperature and oxygen concentration in the period from 16:00 UTC 3.3.2016 until 07:00 UTC 6.3.2016. Note the minimum temperature in the new CIL at the depth range 70-110 m.

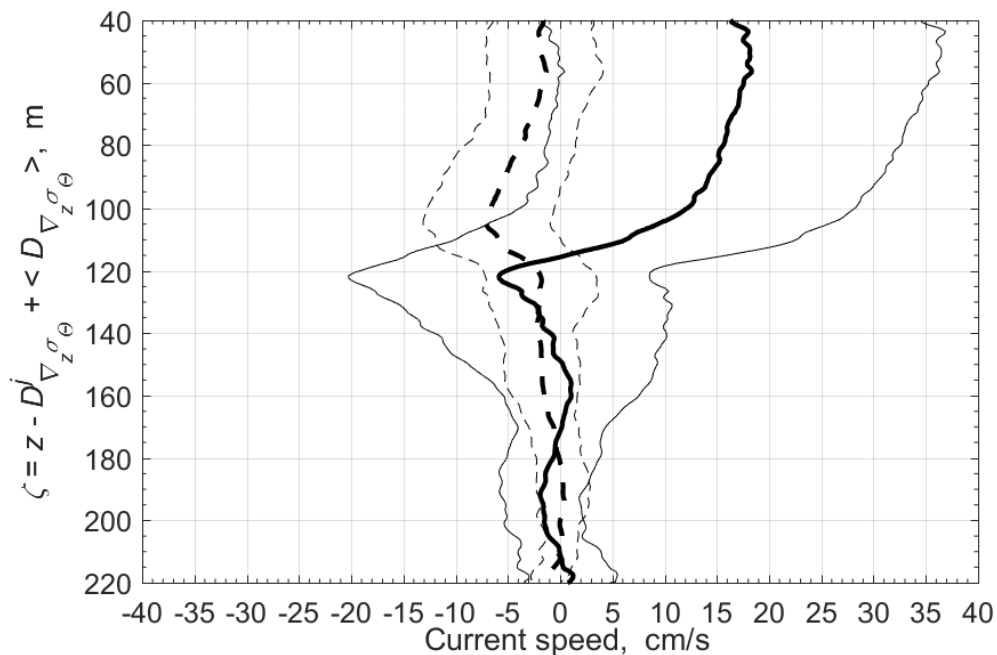


Figure 10: Depth profiles of along-shelf (NW direction is positive; solid curve) and cross-shelf (NE direction is positive; dashed curve) current speed components, which are derived from the ensemble of profiles when $I_{\sigma 14} < 3.5$ mol m⁻² from January-March 2016. The thick curves show the mean profiles, while the thin curves indicate standard deviations.

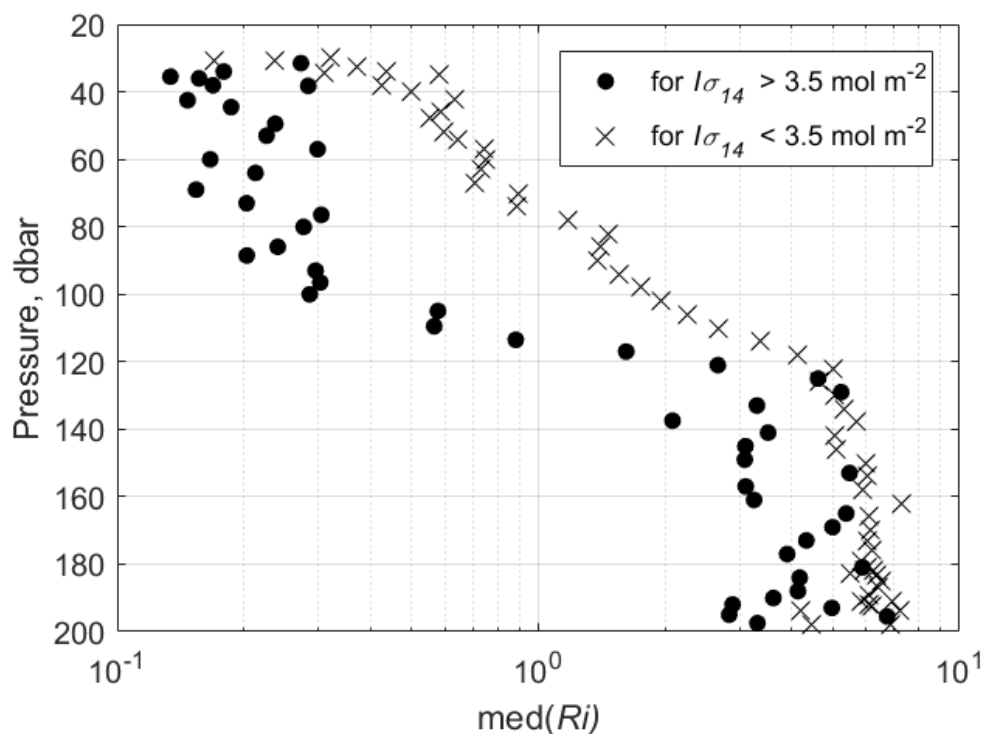


Figure 11: Vertical profiles of the median values of the Richardson numbers that are estimated based on two data ensembles: for $I_{\sigma_{14}} < 3.5 \text{ mol m}^{-2}$ and $I_{\sigma_{14}} \geq 3.5 \text{ mol m}^{-2}$.